Results in Physics 13 (2019) 102236

Contents lists available at ScienceDirect

Results in Physics

journal homepage: www.elsevier.com/locate/rinp

Improving the combination of electrical conductivity and tensile strength of Al 1070 by rotary swaging deformation

Yue Yang, Jinfeng Nie*, Qingzhong Mao, Yonghao Zhao*

Nano and Heterogeneous Materials Center, School of Materials Science and Engineering, Nanjing University of Science and Technology, Nanjing 210094, China

ARTICLE INFO

Keywords:
Aluminum
Rotary swaging
Grain refinement
Strength
Electrical conductivity

ABSTRACT

In the present study, Al 1070 wires were subjected to rotary swaging (RS) with various strains at room temperature. The effect of RS on the microstructure, mechanical property and electrical conductivity was investigated by EBSD, TEM, micro hardness and tensile tests. The results showed that the grains of Al 1070 have been significantly refined and elongated during RS deformation and a fibrous structure has been formed. The elongated grains are mainly composed of sub-grains, which have a high fraction of low angle grain boundaries (LAGBs) up to 75%. Meanwhile, the volume fraction of ⟨1 1 1⟩ fiber texture components increased during RS processing. Due to the refined microstructure, the microhardness and the tensile property of the Al 1070 wires were increased by 54% and 70% after RS deformation at an equivalent strain of ~2. Meanwhile, the combination of the tensile strength and electrical conductivity was improved dramatically. The electrical conductivity of the Al 1070 wires decreased gradually to 56.7% IACS from 58.6% IACS, which is only 1.9% IACS lower than the as-received one. It is proved that grain morphology of the Al wires plays a critical role in controlling the strength-electrical conductivity relation.

Introduction

Pure Al and its alloys are widely applied in the overhead conductor wires, owing to their good electrical conductivity, excellent corrosion resistance, low density, high specific strength and lower cost [1,2]. Achieving high strength and good electrical conductivity in metallic metals is always the aspiration in electrical industry, which supplies the insurance for safety and energy saving. However, the relatively low strength of aluminum limits its application seriously. Furthermore, strength and electrical conductivity are always mutually exclusive in metallic conductive materials. Therefore, an optimum combination of conductivity and tensile strength for aluminum wires is required for use.

In order to increase the strength of the metallic materials, the main strengthening mechanisms have been reported and utilized including grain boundary strengthening (Hall-Petch effect), dislocation strengthening, precipitation strengthening and solid solution strengthening [3–8]. However, all these factors which increase the strength of the alloy tend to cause lattice distortion to different extent and decreases the electrical conductivity correspondingly because of the scattered conducting electrons [9,10]. Usually, solute atoms are widely recognized as having the most harmful effect on electrical conductivity, whereas grain boundaries may be considered as the least efficient lattice defects on scattering electrons in metals [11]. Thus, grain refinement down to sub-micron or nano-scale is an efficient approach to increase the mechanical strength without significant degradation on electrical conductivity [12].

Grains of metals can be significantly refined by subjecting the materials to severe plastic deformation (SPD) processes and the most significant advantage of SPD processes is their ability to effectively enhance physical and mechanical properties of the initially coarse-grained metal via effectively grain refinement process and imposing high amounts of shear strain [13,14]. Al alloys with enhanced strength were obtained using various severe plastic deformation methods such as equal channel angular pressing (ECAP) [15], high-pressure torsion (HPT) [1,16], accumulative roll-bonding (ARB) [17] and twist channel angular pressing (TCAP) [18]. However, the samples of the above methods are always too small to be applied on conductor wires. Meanwhile, the actual production processes of aluminum wires, such as drawing and extrusion, have high energy consumption, poor product quality and limited ability to refine grains. Thus, a reliable, eco-friendly and commercial method still remains to be developed. Rotary swaging (RS), as a relatively new SPD processing technique, can be used to prepare bulk samples including rods, tubes and wires through the repeated action of rotating split dies and then achieves substantial grain refinement [19]. As shown in Fig. 1, there are 4 dies arranged

* Corresponding authors.
E-mail address: niejinfeng@njust.edu.cn (J. Nie).

https://doi.org/10.1016/j.rinp.2019.102236
Received 3 January 2019; Received in revised form 22 March 2019; Accepted 22 March 2019
Available online 27 March 2019

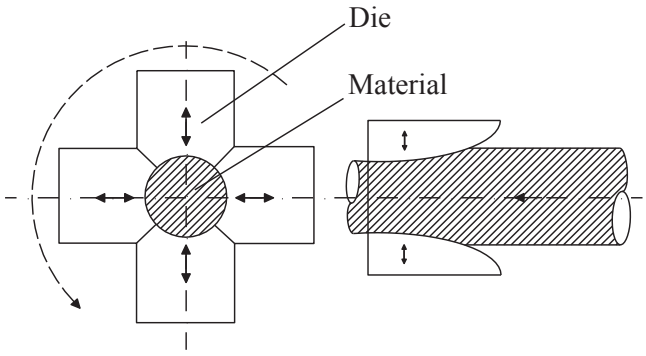

Fig. 1. Schematic diagram of rotary swaging technology.

concentric around the work piece, and these dies move in both radial and axial direction to reduce diameter at a certain position of the work piece or form a concave profile. The advantages of RS also include good surface accuracy, material conservation, and low cost [20].

Even though there are several studies on the microstructure evolution and mechanical properties of the commercial pure aluminum during RS processing, the investigations about its comprehensive effects on the microstructure, strength and the electrical conductivity are still limited. In this work, RS was applied to Al 1070, which aimed to improve the combination of the strength and electrical conductivity. Furthermore, the underlying influence mechanisms of RS on the microstructure, electrical conductivity and mechanical properties of Al 1070 were also explored.

Experimental methods

The experiments were carried out on commercial pure aluminum Al 1070 and the chemical compositions are illustrated in Table 1.

The original aluminum rod with an initial diameter of 30 mm was subjected to RS at ambient temperature with various deformation strains to a final diameter of 11 mm. The equivalent strain induced by RS is defined as:

$$\varepsilon = 2\ln D_0/D \quad (1)$$

where D_0 and D are the diameter of the rod before and after RS, respectively. Four samples were selected with increasing deformation strains, which are named as RS1, RS2, RS3 and RS4, and the specific parameters are shown in Table 2.

Hardness and tensile tests were conducted on the above samples with increasing strains. Vickers hardness (HV) was measured on the cross section of the Al 1070 rods using a HMV-G 21DT (Shimazdu, Japan) equipment at the load of 490 mN and dwelling time of 15 s. The tensile test was tested at room temperature on the WB-LFM 20 KN universal test machine with a constant strain rate of $5 \times 10^{-4}s^{-1}$ according to the ASTM E21 standard and the tensile direction was parallel to the swaging direction. The electrical conductivity was measured at room temperature using a Sigma 2008B digital conductivity meter and at least 30 measurements were taken to obtain the average value as a relative value of the International Annealed Copper Standard (%IACS).

Microstructures of the RS processed specimens were analyzed by electron back-scattering diffraction (EBSD) and transmission electron microscopy (TEM). EBSD was used to characterize the grain structure and sub-grain boundary misorientation distribution in the samples.

Table 1
The chemical composition (wt%) of AA 1070.

Al	Si	Fe	Cu	Mn	Mg	Zn	Ti
99.7	0.11	0.18	0.02	0.014	0.01	0.01	0.01

Table 2
The specific parameters of the Al 1070 samples before and after RS deformation.

Condition	As-received	RS1	RS2	RS3	RS4
Diameter (mm)	30	23.4	18.2	14.2	11
Area reduction (%)	0	39.2	63.2	77.6	86.6
Equivalent strain	0	0.5	1	1.5	2

Specimens for EBSD studies were first mechanically ground up to 1000-grit SiC paper and subsequently electrolytic polished for 15 s at 20 °C and a voltage of 20 V in an etching solution containing 10% perchloric acid and 90% alcohol by volume. The EBSD measurements were carried out by using a Zeiss Auriga field emission scanning electron microscope (SEM) equipped with an Oxford HKL Channel 5 system. TEM observations were also carried out using JEOL 2000EX transmission electron microscope operating at 200 kV. For this purpose, specimens of 3 mm diameter were obtained by punching, grounding down to a thickness of 70 μm and finally twin-jet electropolishing with a solution containing 33% nitric acid and 67% methanol at a voltage of 35 V and a temperature of −35 °C.

Results

Microstructure characterization

To investigate the influence of RS processing on the structural evolution, an EBSD analysis was conducted. Orientation distribution maps and inverse pole figures presented in Fig. 2 show the microstructures and textures of the Al 1070 before and after RS processing with an equivalent strain of 2, respectively. We can see from Fig. 2a that the microstructure of as-received material consists of a relatively coarse grain size of about 150 μm. After RS processing, the fibrous structures along the swaging direction replace the original equiaxed grains. The adjacent grain boundaries consisting of HAGBs are almost parallel to each other and the thickness of the elongated grains is used to denote the grain size which is about 20 μm as shown in Fig. 2c. Therefore, a significant grain refinement has been achieved after RS processing for an equivalent strain of 2. Furthermore, it can be observed that the unprocessed Al sample exhibited more or less random grains orientations, having ⟨0 0 1⟩ texture as the preferential orientation. During the RS processing, the grains of ⟨0 0 1⟩ orientation tend to be reduced in quantity and gradually rotate towards ⟨1 1 1⟩ orientation and the mainly texture components are strong ⟨0 0 1⟩ and ⟨1 1 1⟩ fiber textures, which are the typical ones in the face-centered-cubic (FCC) metals after cold deformation [21].

To investigate the densities of the different types of boundaries, the grain boundary map for the EBSD data is presented in Fig. 3a with corresponding misorientation angle distribution histogram in Fig. 3b for the sample after RS processing with an equivalent strain of 2. In the grain boundary map, boundaries are presented as fine red lines for low angle grain boundaries (misorientation angle of 2–15°, LAGBs) and high angle grain boundaries (misorientation angle exceeding 15°, HAGBs) are presented as thick black lines. As shown in Fig. 3b, it can be seen that the misorientation angle is mainly distributed at 2–15° after RS processing with a high fraction of LAGBs of 75%. The high fraction of LAGBs means that a large number of sub-boundaries are formed by the dislocation tangle during the RS deformation and the elongated grains are mainly composed of sub-grains.

TEM was further used to analysis the grain structure of the sample in its cross and longitudinal sections after RS processing as shown in Fig. 4. The bright-field image in Fig. 4a shows that the microstructure in the cross section normal to the swaging directions composed of a large number micron sized grains. It is obvious at high magnification in Fig. 4b that the ill-defined boundaries of these grains are formed by

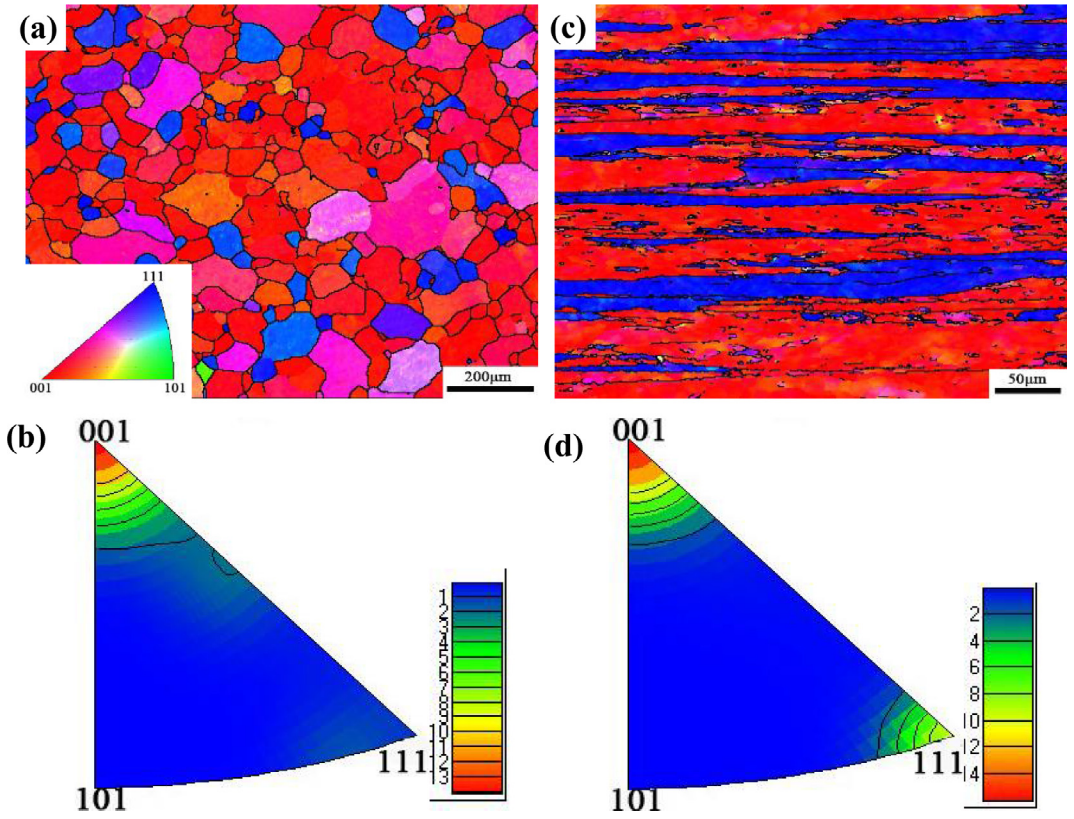

Fig. 2. The orientation distribution maps and inverse pole figures of the (a, b) as-received and (c, d) RS processed Al 1070 with an equivalent strain of 2.

dislocation tangle and these small grains are sub-grains. Along the swaging direction in the longitudinal section, many bands of elongated substructures can be observed in Fig. 4c, d. It is also noted that a relatively low density of lattice dislocations can be seen in the grain interior and most of grains are very clean indicating the occurrence of dislocation recovery during RS deformation. As the stacking fault energy of aluminum alloy is relatively high and the self-diffusion energy is less, dislocations are easier to recover due to the dominating wavy slip mode [22,23].

Mechanical properties and electrical conductivity

The microhardness and tensile strength of the Al wires before and after swaging with different equivalent strains are shown in Fig. 5. As shown in Fig. 5a, the microhardness of as-received material was ~25.6 HV and it increased with the increasing strain. At an equivalent strain of 2, it reached up to ~39.5 HV, 54% higher than that of the as-received one. The engineering stress–strain curves of the samples with different deformation strains are shown in Fig. 5b. It can be seen that the yield and tensile strength were also greatly enhanced at $\varepsilon = 2$ which increased by 194% and 70%, respectively. However, the elongation decreased dramatically after RS processing, which is consistent with typical strength and ductility tradeoff relationship.

Fig. 6 illustrates the fracture surfaces of the as received and RS processed Al 1070 samples after tensile tests to investigate the failure mechanism. A typical ductile fracture with a large number of dimples can be seen in the as-received sample (Fig. 6a). However, the dimple size decreased slightly after RS processing and shear zones can be seen as shown in Fig. 6b.

The measured electrical conductivities of the Al wires before and after RS are presented in Table 3. It can be seen that electrical conductivity of the as-received material equaled to 58.6%IACS. The

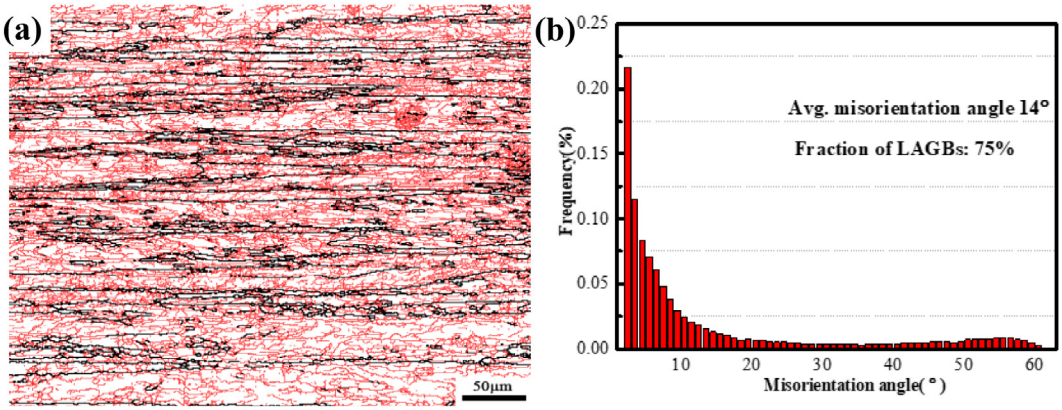

Fig. 3. (a) Grain boundary map; (b) Histogram of the variation of misorientation angle of the RS processed Al 1070 with an equivalent strain of 2.

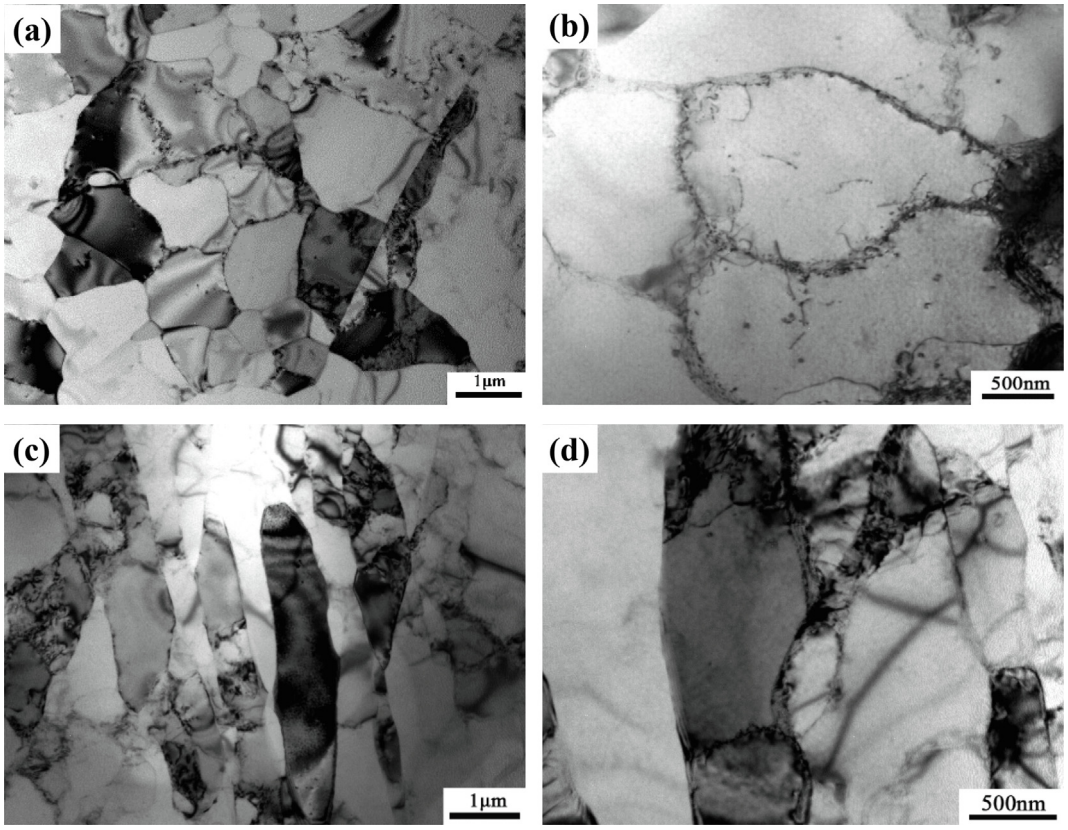

Fig. 4. TEM bright field micrographs for RS processed sample (a, b) normal (c, d) parallel to the swaging direction.

electrical conductivity of the samples decreased gradually with increasing RS deformation strain. However, it decreased to 56.7% IACS when accumulated strain reaches about 2, which is only 1.9% IACS lower than the as-received sample.

The tensile strength and electrical conductivity values of Al1070 alloy after different deformation strains are plotted as a function of equivalent strains illustrated in Fig. 7. The curves suggest that RS processing leaded to a significant increase of the strength, whilst a slight decrease of the electrical conductivity. The reduction in electrical conductivity is only 1.9% IACS when the accumulative equivalent strain is bout 2, while the tensile strength increased by 70% compared with the as-received material. Therefore, the combination of the tensile strength and electrical conductivity has been improved dramatically after RS processing.

Discussion

Based on the above analysis, it can be seen that the microstructure of the Al 1070 wires has been refined significantly during the RS deformation. Meanwhile, the strength and electrical conductivity of the samples varied with the development of the microstructure. Grain structure, dislocation, texture are the main microstructure characteristics in the present samples. As shown in Fig. 4, the density of dislocations in the RS processed samples keeps in a relatively low level, because the dislocations tend to recover during the deformation due the relatively high stacking fault energy of Al. However, the types of texture and the characteristics of grains changed obviously with the increasing deformation strain. Therefore, the grain boundary strengthening and texture strengthening should play a significant role during the RS processing.

According to the Hall-Petch relation, grain refinement can

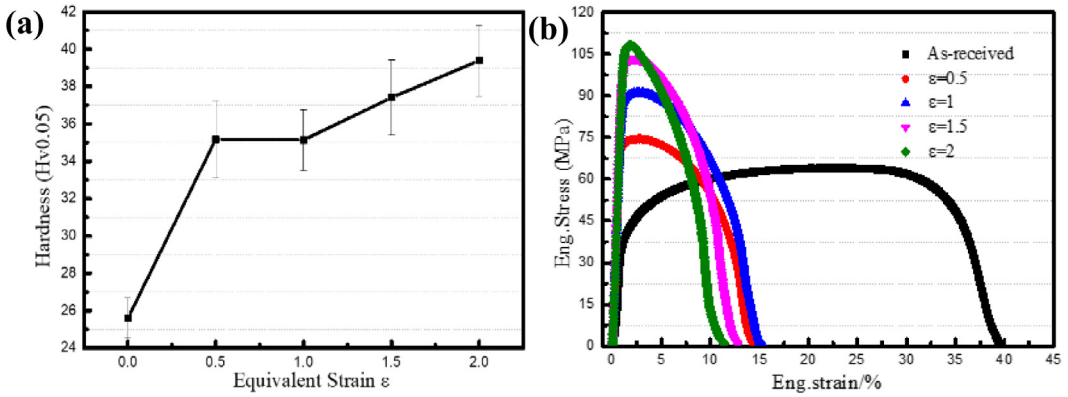

Fig. 5. (a) Microhardness and (b) Engineering stress–stain curves of the Al wires before and after RS processing with various strains.

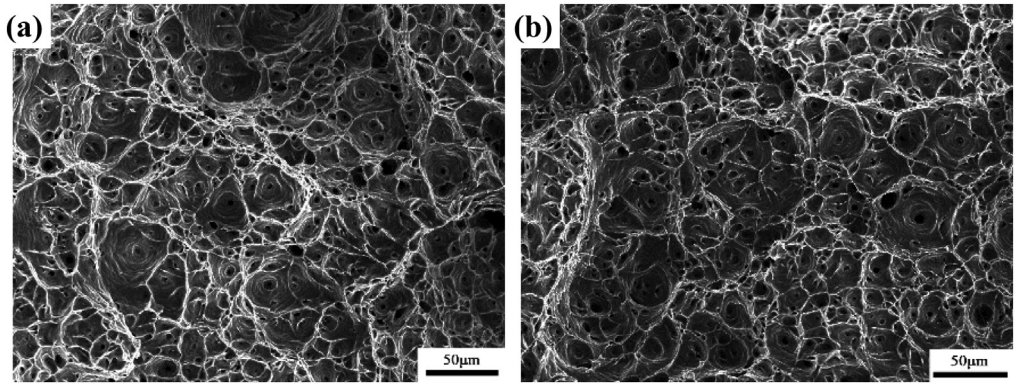

Fig. 6. Fracture surfaces for (a) as-received (b) RS processed Al 1070.

Table 3
Electrical conductivities of the Al 1070 Al samples before and after RS.

Strain	0	0.5	1	1.5	2
Measured Electrical conductivity (%IACS)	58.6	58.5	58.2	57.8	56.7

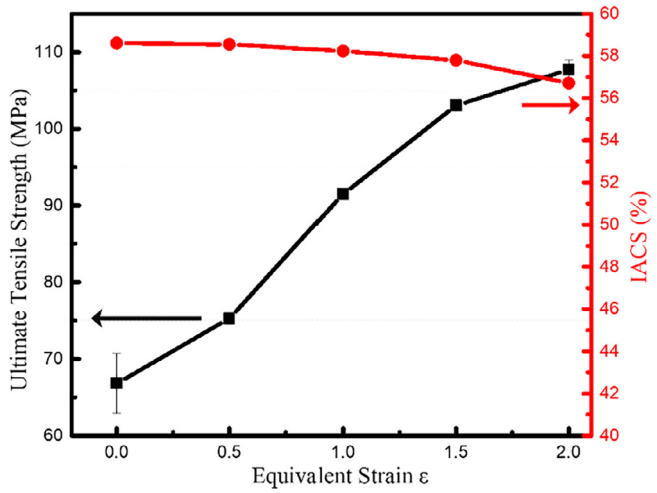

Fig. 7. Tensile strength and electrical conductivity variation with deformation strain.

effectively improve the mechanical properties of metals. In the present study, grains of Al wires have been elongated and refined significantly, which also contain a large number of sub-boundaries. It is well known that grain boundary can effectively hinder the movement of the dislocations and strengthen the materials [24]. Furthermore, the contribution of LAGBs to strength of materials can be regarded as HAGBs [25,26], which can be described by the following equation:

$$\sigma_s = \sigma_0 + kd^{-1/2} \quad (2)$$

where σ_s is the yield strength, d is the grain size, σ_0 and k are the constants equal to 20 MPa and 40 MPa μm½ for aluminum [27]. In this study, the smaller grain size and the higher density of LAGBs can effectively strengthen the strength of Al 1070. Taking LAGBs into account, the grain size is about 1 μm and the contribution to yield strength is about 60 MPa, accounting for 86% of the increase in yield strength, which means that the grain boundary strengthening is the main contribution to the strength.

In addition, texture strengthening also contributes to the improvement of the tensile strength. The orientation distribution maps in Fig. 2 show that the volume fraction of ⟨1 1 1⟩ fiber texture components increased during the RS processing. Furthermore, the ⟨1 1 1⟩ orientation has been reported as 'harder' orientation compared with ⟨0 0 1⟩ orientation, because the Schmid factor (SF) of ⟨1 1 1⟩ is smaller than that of ⟨0 0 1⟩, which equal to 0.272 and 0.408, respectively [28,29]. According to the Schmid law, the decrease of SF indicates that the resolved shear stress acting on the slip system decreases and then larger external stress is needed to activate the slip system. Therefore, the strength of ⟨1 1 1⟩ oriented grains is always higher than that of ⟨0 0 1⟩ oriented ones. Hence, the increase of ⟨1 1 1⟩ texture during the RS processing also contributes to the improvement of the tensile strength to some extent. Meanwhile, grains in ⟨1 1 1⟩ texture with lower SF are harder to activate slip during deformation, leading to the exhaustion of plasticity.

As it is well known that, all strengthening factors lead to an additional distortion in the lattice, which can provide an additional increase of electrical resistivity of metallic materials [30], and the well-known Matthiessen's rule can be expressed as [31]:

$$\rho_{total} = \rho + \rho_{ss} + \rho_p + \rho_d + \rho_{gb} \quad (3)$$

where ρ_{total} is the total electrical resistance, ρ is the electrical resistivity of the lattice, ρ_{ss} is the resistivity due to solute atoms dissolved in the matrix, ρ_p is the resistivity added by second-phase precipitates, ρ_d is the resistivity due to dislocations existed in the microstructure, ρ_{gb} is the resistivity due to grain boundaries. In this study, the effect of solute atoms and second-phase precipitates on the variation of electrical conductivity can be neglected and the effect of dislocations is also can be ignored due to the recovery of dislocations. It is evident that the grain size decreased significantly after RS processing, and then grain boundaries should dominate the change of electrical conductivity in the Al 1070 wires during the RS processing. Previous studies on pure Cu and Al alloys have demonstrated that grain refinement can improve mechanical strength of pure metals without much sacrifice of their electrical conductivity [32]. It is due to the fact that the grain size is much larger than the electron mean free path, so the boundary contribution to the electrical resistivity can be regarded as negligible. Besides, grains are elongated along the RS direction and a fibrous texture is formed on the longitudinal section. On one hand, the thin and long fibrous structure with a large number of sub-grain boundaries can improve the strength caused by the Hall-Petch effect. On the other hand, the elongated grain boundaries parallel to the direction of current, which is beneficial to the electron transporting and significantly reduces the interfacial scattering. Therefore, the reduction of electrical conductivity induced by the grain boundaries is very limited, compared with its substantial contribution to the increase of strength. The variation of the electrical conductivity and strength for the samples before and after RS processing in Fig. 7 also shows a good accordance with the microstructure evolution.

Based on the above results and discussion, it suggests that the grain morphology in the CP Al conductor must be a critical factor controlling the strength-electrical conductivity relation, which can be used to

fabricate CP Al conductor with high strength and good conductivity. RS processing is also proved to be an effective method to improve the strength of aluminum wires without much sacrifice of the electrical conductivity. In addition, RS can be used to produce bulk conductive wires with various diameters in a progressive way and can be directly applied to industrial production, which shows its superiority compared with other traditional SPD methods with limited sample size.

Conclusions

In this study, Al 1070 was subjected to RS processing with various strains and the effect of RS on the mechanical property and electrical conductivity were investigated. The following conclusions could be drawn as:

(1) The grains of Al 1070 have been significantly refined and elongated during RS deformation and a fibrous structure has been formed. The average thickness of the grains has been reduced to about 20 μm after RS processing for an equivalent strain of about 2. The elongated grains are mainly composed of lots of sub-grains, which leads to the increase of low angle grain boundaries (LAGBs) up to 75%. Meanwhile, the grains of ⟨0 0 1⟩ orientation tend to be reduced in quantity and gradually rotate towards ⟨1 1 1⟩ orientation.
(2) The microhardness of the Al 1070 wires increased with increasing equivalent strain during RS processing and reached up to 39.5 HV when the equivalent strain equals 2, 54% higher than that of the as-received one. The tensile strength was also significantly improved by 70% and increased to 109 MPa from 65 MPa after RS processing, while the elongation showed a dramatic decrease.
(3) The combination of the tensile strength and electrical conductivity has been improved dramatically after RS processing. The electrical conductivity of the Al 1070 wires decreased gradually to 56.7% IACS when accumulated strain reaches about 2, which is only 1.9% IACS lower than the as-received sample.
(4) It is proved that the elongated grain boundaries parallel to the direction of current, which is beneficial to the electron transporting. Therefore, the increased grain boundaries lead to a small reduction of electrical conductivity, whilst a significant contribution to the increase of strength.

Acknowledgements

This work is supported by the National Key R&D Program of China (No. 2017YFA0204403) and the Natural Science Foundation of China (Nos. 51731007 and 51501092 and 2012CB932203). The authors also want to acknowledge the support of the Jiangsu Key Laboratory of Advanced Micro-Nano Materials and Technology. SEM, TEM and EBSD experiments are performed at the Materials Characterization and Research Center of Nanjing University of Science and Technology.

References

[1] Valiev RZ, Murashkin MY, Sabirov I. A nanostructural design to produce high strength Al alloys with enhanced electrical conductivity. Scr Mater 2014;76:13–6.
[2] Sauvage X, Bobruk EV, Murashkin MY, Nasedkina Y, Enikeev NA, Valiev RZ. Optimization of electrical conductivity and strength combination by structure design at the nanoscale in Al-Mg-Si alloys. Acta Mater 2015;98:355–66.
[3] Carlton CE, Ferreira PJ. What is behind the inverse Hall-Petch effect in nanocrystalline materials? Acta Mater 2007;55:3749–56.
[4] Bannaravuri PK, Birru AK. Strengthening of mechanical and tribological properties of Al-4.5%Cu matrix alloy with the addition of bamboo leaf ash. Results Phys 2018;10:360–73.
[5] Ma KK, Wen H, Hu T, Topping TD, Isheim D, Seidman DN, et al. Mechanical behavior and strengthening mechanisms in ultrafine grain precipitation-strengthened aluminum alloy. Acta Mater 2014;62:141–55.
[6] Gupta AK, Lloyd DJ, Court SA. Precipitation hardening in Al-Mg-Si alloys with and without excess Si. Mater Sci Eng, A 2001;316:11–7.
[7] Seidman DN, Marquis EA, Dunand DC. Precipitation strengthening at ambient and elevated temperatures of heat-treatable Al(Sc) alloys. Acta Mater 2002;50:4021–35.
[8] Fribourg G, Brechet Y, Deschamps A, Simar A. Microstructure-based modelling of isotropic and kinematic strain hardening in a precipitation hardened aluminium alloy. Acta Mater 2011;59:3621–35.
[9] Murashkin MY, Sabirov I, Sauvage X, Valiev RZ. Nanostructured Al and Cu alloys with superior strength and electrical conductivity. Mater Sci 2016;51:33–49.
[10] Guan RG, Shen YF, Zhao ZY, Wang X. A high-strength, ductile Al-0.35Sc-0.2Zr alloy with good electrical conductivity strengthened by coherent nanosized-precipitates. J Mater Sci Technol 2017;33:215–23.
[11] Rositter PL. The electrical resistivity of metals and alloys. Cambridge: Cambridge University Press; 1991.
[12] Hall EO. The deformation and aging of mild steel. Proc Phys Soc 1951;64:747–53.
[13] Kocich R, Kunčická L, Král P, Macháčková A. Sub-structure and mechanical properties of twist channel angular pressed aluminium. Mater Charact 2016;119:75–83.
[14] Li JS, Cao Y, Gao B, Li YS, Zhu YT. Superior strength and ductility of 316L stainless steel with heterogeneous lamella structure. J Mater Sci 2018;53:10442–56.
[15] Tolaminejad B, Dehghani K. Microstructural characterization and mechanical properties of nanostructured AA1070 aluminum after equal channel angular extrusion. Mater Des 2012;34:285–92.
[16] Mavlyutov AM, Bondarenko AS, Murashkin MY, Boltynjuk EV, Valiev RZ, Orlova TS. Effect of annealing on microhardness and electrical resistivity of nanostructured SPD aluminium. J Alloy Compd 2017;698:539–46.
[17] Miyajima Y, Komatsu SY, Mitsuhara M, Hata S, Nakashima H, Tsuji N. Microstructural change due to isochronal annealing in severely plastic-deformed commercial purity aluminium. Phil Magn 2015;95:1139–49.
[18] Kunčická L, Kocich R, Král P, Pohludka M, Marek M. Effect of strain path on severely deformed aluminium. Mater Lett 2016;180:280–3.
[19] Abdulstaar MA, El-Danaf EA, Waluyo NS, Wagner L. Severe plastic deformation of commercial purity aluminum by rotary swaging: microstructure evolution and mechanical properties. Mater Sci Eng, A 2013;565:351–8.
[20] Wang HF, Han JT, Hao QL. Fabrication of laminated-metal composite tubes by multi-billet rotary swaging technique. Int J Adv Manuf Technol 2014;76:713–9.
[21] Han K, Vasquez AA, Xin Y, Kalu PN. Microstructure and tensile properties of nanostructured Cu-25wt%Ag. Acta Mater 2003;51:767–80.
[22] An XH, Wu SD, Wang ZG, Zhang ZF. Enhanced cyclic deformation responses of ultrafine-grained Cu and nanocrystalline Cu-Al alloys. Acta Mater 2014;74:200–14.
[23] Huang F, Tao NR, Lu K. Effects of impurity on microstructure and hardness in pure Al subjected to dynamic plastic deformation at cryogenic temperature. J Mater Sci Technol 2011;27(7):628–32.
[24] Cabibbo M. Microstructure strengthening mechanisms in different equal channel angular pressed aluminum alloys. Mater Sci Eng, A 2013;560:413–32.
[25] Kamikawa N, Huang XX, Tsuji N, Hansen N. Strengthening mechanisms in nanostructured high-purity aluminium deformed to high strain and annealed. Acta Mater 2009;57:4198–208.
[26] Hansen N. Boundary strengthening in undeformed and deformed polycrystals. Mater Sci Eng, A 2005;409:39–45.
[27] Gashti SO, Fattah-alhosseini A, Mazaheri Y, Keshavarz MK. Effects of grain size and dislocation density on strain hardening behavior of ultrafine grained AA1050 processed by accumulative roll bonding. J Alloy Compd 2016;658:854–61.
[28] Beyerlein IJ, Tóth LS. Texture evolution in equal-channel angular extrusion. Prog Mater Sci 2009;54:427–510.
[29] Hou JP, Wang Q, Yang HJ, Wu XM, Li CH, Li XW, et al. Microstructure evolution and strengthening mechanisms of cold-drawn commercially pure aluminum wire. Mater Sci Eng, A 2015;639:103–6.
[30] Lu L, Shen YF, Chen XH, Qian LH, Lu K. Ultrahigh strength and high electrical conductivity in Copper. Science 2004;304:422–6.
[31] Matthiessen A, Vogt C. On the influence of temperature on the electric conducting-power of thallium and iron. Proc R Soc London 1862;12:472–5.
[32] Luo XM, Song ZM, Li ML, Wang Q, Zhang. GP. Microstructural evolution and service performance of cold-drawn pure aluminum conductor wires. Mater Sci Technol 2017;33:1039–43.